Biometals (2009) 22:197–205
DOI 10.1007/s10534-008-9200-5

Quantitative imaging of metals in tissues

Martina Ralle · Svetlana Lutsenko

Received: 13 November 2008 / Accepted: 10 December 2008 / Published online: 7 January 2009

Abstract Metals and other trace elements play an important role in many physiological processes in all biological systems. Characterization of precise metal concentrations, their spatial distribution, and chemical speciation in individual cells and cell compartments will provide much needed information to explore the metallome in health and disease. Synchrotron-based X-ray fluorescent microscopy (SXRF) is the ideal tool to quantitatively measure trace elements with high sensitivity at high resolution. SXRF is based on the intrinsic fluorescent properties of each element and is therefore element specific. Recent advances in synchrotron technology and optimization of sample preparation have made it possible to image metals in mammalian tissue with submicron resolution. In combination with correlative methods, SXRF can now, for example, determine the amount and oxidation state of trace elements in intra-cellular compartments and identify cell-specific changes in the metal ion content during development or disease progression.

Keywords Synchrotron-based X-ray fluorescence · Metallome · Metal imaging · Elemental maps · Submicron resolution

M. Ralle (✉) · S. Lutsenko
Department of Biochemistry and Molecular Biology, Oregon Health & Science University, 3181 SW Sam Jackson Park Rd, Portland, OR 97239-3098, USA
e-mail: rallem@ohsu.edu

Introduction

Trace elements like Fe and Cu are essential in numerous biochemical processes in virtually all organisms from bacteria to man. Most organisms have developed specific mechanisms by which they regulate uptake and excretion, intracellular translocation, and compartmentalization of metals. These mechanisms are necessary to protect cells from an often toxic reactivity of elements like Fe and Cu while simultaneously ensuring proper availability. Disruption of metal ion uptake and/or proper distribution leads to a variety of human disorders (Choi and Koh 1998; Danks et al. 1972; Koh et al. 1996; Loudianos and Gitlin 2000; Waggoner et al. 1999). Comprehensive mechanistic understanding of pathologies associated with metal misbalance requires not only knowledge of the biochemical processes in which metal ions are involved but also our ability to accurately detect elemental species in cells and tissues as well as the means to characterize changes in their concentration, oxidation state, and ligand-coordination environment. Thus, the biology of cells in health and disease can only be understood through systematic analysis of their genome, proteome, and their metallome, with the latter providing information about the distribution and abundance of metals in cellular compartments and individual molecules. Extracting the functional connections between genes, proteins, metabolites and trace metal ions is an important and exciting challenge in the post-genomic

area (Lahner et al. 2003). The analysis of trace elements in cells and tissues is dependent on the availability of methods that have sufficient selectivity, sensitivity, and resolution to extract quantitative data about metal ions when analyzed against the background of numerous other cell components. Technological advances in the past 10 years have made studies of distribution, concentration, speciation, as well as biochemical function of metals in biological materials possible. The purpose of this review is to provide an overview of these methods with emphasis on recent advances in X-ray fluorescence microscopy, and utilization of this technology as a tool to image trace elements in healthy and diseased mammalian tissue.

Challenges of measuring metal concentrations in biological material

Recent developments of high resolution technologies to image metals have aimed to accomplish two goals: to enable reliable measurements of metals with subcellular resolution and to identify changes in metal concentration, localization, and/or oxidation state that accompany pathology development and can therefore serve as prediction of a disease state (i.e. metallo biomarkers). Which experimental approach is used to evaluate metals in a biological setting depends mostly on the desired resolution (for example different methods are needed to measure bulk metal concentrations in tissue compared to spatially resolved measurements in cells or in cellular organelles), number of samples, and whether the integrity of biological material needs to be preserved for additional analyzes.

Concentrations of trace elements are often accessed by bulk chemical analysis such as atomic absorption spectroscopy (AAS) or inductively coupled plasma mass spectroscopy (ICP-MS). Although both methods are very sensitive (parts per billion (AAS) or parts per trillion (ICP-MS)), all spatial information is lost due to homogenization of the material prior to measurements. In order to study 2-dimensional (2-D) distributions of metals in tissues and cells, investigators had to rely solely on histological methods until recently. These procedures employ either a colored compound (dye) or a fluorescently labeled chemical, which when applied to tissue undergo a chemical reaction and precipitate (color stains) or form a stable chemical complex (fluorescence labels) with the metal. The success of these methods strongly depends on sample preparation and preservation, during which weakly bound metals can diffuse out of cells or tissue. Furthermore, the specificity and reactivity of the complex-forming chemical reaction that ultimately determine the sensitivity these methods are often unknown. Thus, even if a metal is abundant in tissue it may not be detected unless its oxidation state and coordination environment favor complex formation with the dye or fluorescent label.

A typical example is given in Fig. 1. Here, we are comparing concentration and distribution of copper in hepatic tissue from an explanted liver of a Wilson disease (WD) patient to that of *Atp7b*$^{-/-}$ mice, a mouse model for WD (Buiakova et al. 1999;

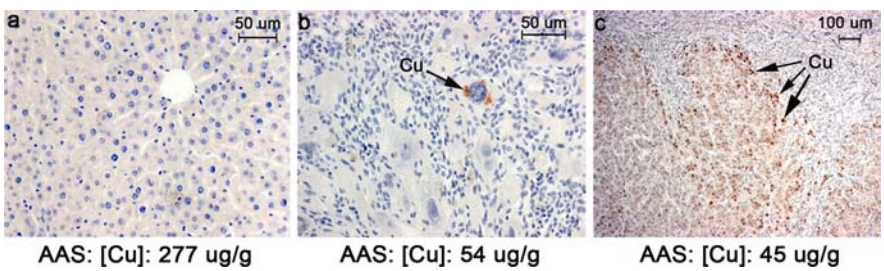

Fig. 1 Comparison of traditional copper detection methods and SXRF. **a** 6-week old, pre-symptomatic; **b** 20-week old Atp7b$^{-/-}$ liver, advanced disease state; **c** late stage WD, human tissue section stained with rhodanine and bulk copper concentration from AAS (copper concentration is given as wet weight). The rhodanine stain was negative at the pre-symptomatic stage (staining grade 0; **a**), weak in livers from a 20-week old mouse (staining grade 1; **b**), and medium in a human liver sample at the late stages of WD (staining grade 2; **c**). The AAS results did not correlate with the histochemical findings, the bulk copper concentration was highest at 6 weeks (where no staining is observed) and about equal in samples from the advanced stages of the disease

Huster et al. 2006). WD is a genetic disorder in which copper accumulates to high levels in tissues, particularly in the liver (Ala et al. 2007; Loudianos and Gitlin 2000). The bulk copper concentration was assessed by AAS from homogenized tissue while the spatial copper distribution was evaluated by rhodanine staining of paraffin embedded tissue sections. It can be clearly seen that the histology results do not reflect the total levels of copper in tissue. High levels of copper in a 6-week old mouse liver (227 μg/g wet weight, as measured in a liver homogenate by AAS) are not detected with rhodanine in a tissue section that originated from the same liver (Fig. 1a). In stark contrast, a section of tissue from a WD patient that exhibited lower copper levels in the bulk homogenate (54 μg/g wet weight) clearly demonstrated discrete copper deposits (Fig. 1c). Hepatic tissue from a 20-week old *Atp7b*$^{-}$/$^{-}$ mouse with a medium copper concentration showed a few copper deposits (Fig. 1b). These differences in sensitivity of AAS and rhodanine staining are not due to differences between mice and human, but rather the form in which copper is present at the earlier and later stage of WD. Hence, to reliably detect metals in tissues it is important to use methods that are independent of the chemical state as well as sensitive enough to detect low local concentration of the metal. Synchrotron-based X-ray fluorescence (SXRF) is the ideal tool to measure multiple metals independently of their chemical state and environment; SXRF will be described in later sections in detail.

Methods to image trace metals in biological material with spatial resolution

A number of spectroscopic techniques that are based on specific atomic properties are currently available to image trace elemental distribution thereby complementing the bulk analyses by AAS. Table 1 lists the major techniques and their characteristic features.

Electron microprobe (EM) uses an energy dispersive detector with a transmission electron microscopy (Roomans 1988; Roomans and Von Euler 1996). In this method, an electron beam is used to excite outer shell electron of atoms which upon re-arrangement emits X-rays. The energy of the emitted X-rays is element specific and can be used to determine the elemental composition of a biological sample with an energy dispersive detector. However, electrons generate a significant amount of Bremsstrahlung (radiation caused by decelerations of charged particles when passing through the field of nuclei), which lowers the sensitivity for trace elements (Sparks 1980). Current sensitivity of EM in thin sections is between 100 and 1,000 μg/g. An important issue to consider when working with EM is side-scattering, that can increase the excited area to more than 100 nm^2 irrespective of the size of the electron beam (Kirz et al. 1978). In addition, EM requires lengthy sample preparation which is necessary to preserve tissue morphology at nm resolution. However, dehydration and embedding of EM samples potentially allow for weakly bound metals to diffuse out of the sample. A compromise is to perform cryo-EM and use

Table 1 Major spatially resolved methods to image trace elements in biological material (adapted from {Lobinski, 2006 #235})

Technique	Analytical depth (μm)	Spatial resolution (μm)	Technique	Quantification	Destructive	Instrument
Electron microprobe	0.1–100	30 nm	Elemental imaging	Quantitative	No	Transmission electron microscope with electron microprobe
Laser ablation microscopy coupled with ICP-MS	1–200	12–20 μm	Elemental imaging	Quantitative	Yes	Laser ablation microscope in combination with ICP-MS
SXRF	>500	0.1–1 μm	Elemental imaging	Quantitative	No	Synchrotron source
μ-XANES	>500	0.1 μm	Chemical speciation		No	Synchrotron source

specimen that were flash-frozen in liquid ethane. The freezing process will produce thin layers of hydrated, frozen material in which cellular structure and elemental composition are perfectly preserved. Despite these limitations electron microprobe can measure all major trace elements (with $z \geq 6$) in biological specimen (Hanaichi et al. 1984; Laquerriere, 2002 #244; Zierold 2000). It can be successfully used when metals are tightly bound and the identification of intracellular compartments is critical.

Micro-particle induced X-ray emission (*μ-PIXE*) uses a focused ion beam (1–5 μm^2 cross section) instead of an electron beam which increases the sensitivity of measurements by 100-fold (detection limit 1–10 μg/g). Particles for *μ*-PIXE are less easy to generate than electrons but their relatively higher momentum produces less Bremsstrahlung and side-scattering. (Kirz et al. 1978). Like electron microprobe, PIXE can simultaneously measure all elements ($z \geq 6$) if used in combination with an energy dispersive detector. PIXE has an acceptable penetration depth of ~100 μm but cannot be used for chemical speciation (for a review see (Szokefalvi-Nagy 1994)). For a recent report, describing the evaluation of subcellular distribution of metals in mouse brains *μ*-PIXE see (Nakazato et al. 2008).

Laser ablation inductively coupled mass spectrometry (*LA ICP-MS*) uses a focused laser to evaporate a small area of sample after which the elemental composition of the evaporated material is analyzed by ICP-MS. The resolution of this technique is limited (≥12 μm) and the procedure is destructive to biological material. However, the sensitivity is exceptional (0.01 μg/g) and the instrumentation required for the measurements is less complex. This makes LA ICP-MS more accessible for routine measurements compared to all other methods discussed here. The low resolution renders LA ICP-MS unsuitable for subcellular imaging of metals but makes it the method of choice (in combination with ESI-MS) to identify metalloproteins in complex mixtures that were separated on 2-D electrophoresis gels. (Becker et al. 2008, 2005).

Synchrotron-based X-ray absorption spectroscopy

Synchrotron-based X-ray fluorescence is a rapidly emerging high resolution method to image elements in biological samples. The principle of SXRF is based on the intrinsic fluorescent properties of elements. High energy X-rays (primary radiation) are used to emit inner shell electrons (such as *k*- or *l-shell*) from atoms of an object into the continuum. Outer shell electrons fill the inner shell vacancies, thereby emitting fluorescence (secondary radiation). The energy of these secondary X-rays depends on the properties of the nucleus and the electron shell and is different for each element and/or oxidation state. X-ray fluorescent measurements of biological samples yield quantitative information about the spatial distribution of multiple elements simultaneously with high sensitivity and low background (Yun et al. 1999). No dyes are needed and -when carried out in energy scanning mode- SXRF and can be used to determine the oxidation state of an element. While many X-ray synchrotron sources have focusing optics that achieve resolution in the low micrometer range (for examples see: (McCrea et al. 2008; Miller et al. 2006; Pickering et al. 2006, 2000; Sham et al. 2005)) only third generation synchrotron sources (APS, Argonne, USA; ESRF, Grenoble, France; and SPring8, Hyogo, Japan) can provide high brilliance at high photon energy that is needed to acquire 2-D elemental maps at submicron (~200 nm) resolution. To date, SXRF is the *only* available method for quantitative imaging of whole cells (see Dillon et al. 2002; Hall et al. 2003; Harris et al. 2005; Kemner et al. 2004; McRae et al. 2006; Paunesku et al. 2003; Twining et al. 2003; Waern et al. 2005; Yang et al. 2005).

SXRF imaging in mammalian tissue. Visualizing elemental distribution in biological material other than cells adds another level of difficulty to the experiment. Like in EM and *μ*-PIXE, it is critical that the preservation of tissue morphology is sufficiently high to match the resolution of SXRF, i.e. the visualizing 2-D elemental maps should not be limited by the quality of sample preparation (morphology). SXRF is exceptionally sensitive; attomolar (10–18) amounts of trace elements can be detected in single cells or 10 μm tissue sections (Twining et al. 2003), so even slight losses or re-distribution of elements during tissue preparation and sectioning may lead to incorrect conclusions. In addition, to increase the information content of the SXRF-generated data, one needs to increase the size of the measured sample (areas to be scanned) beyond a

few cells. Similarly, the number of imaged sections should be sufficiently high to obtain statistically significant data. This number is largely determined by the heterogeneity (different cell types) of the scanned tissue.

Spectral analysis in SXRF microscopy

It is important to emphasize that SXRF imaging is a quantitative method. Analysis of the SXRF scans and metal quantification is routinely done at high resolution micro imaging beamlines at the Advanced Photon Source (Argonne, IL; beamlines 2-ID-E and 2-ID-D). For each scan, full X-ray fluorescence spectra are collected at every position during the scan. The spectra are individually fitted using modified Gaussians for fluorescence peak descriptions, and an adapted version of the SNIP algorithm for the determination of background (Van Espen 2002). Absolute quantification is carried out by comparison of fluorescence counts from the sample to a calibration curve based on X-ray fluorescence of the thin film NBS 1,832 (Cu) and 1,833 (Zn) (National Institute of Standards and Technology (NIST) formally National Bureau of Standards (NBS), Gaithersburg, MD).

For the analysis of the average elemental content in specific regions of interest (ROIs), the fluorescent spectra for the respective ROIs are extracted from the original dataset, added up, and fitted and quantified as described above. For each scan, the 3-dimensional elemental maps of energy in x,y 2-D coordinates are created using the software tool MAPS (Vogt 2003). This is done by integrating the fluorescence counts over the energy region of the element's k-edge. For example, the spectral region for copper usually is 8.02–8.07 keV (Cu-Kα_1-line: 8.049 keV). For improved accuracy and to reduce spectral overlap between adjacent K_α emission lines, the spectra are fitted at every pixel individually. Calibration to area densities ($\mu g/cm^2$) is carried out by comparing the fluorescence signal strength of the sample to that of NBS1832 and NBS1833 using MAPS. To obtain elemental concentrations within chosen ROIs, the integrated spectra of these regions are fitted and the resulting fluorescent signal compared to the fitted standard spectra.

Correlative techniques in SXRF imaging

Although, the SXRF imaging is particularly informative when the SXRF-generated elemental 2-D maps are correlated with tissue and cellular morphology, achieving such close correlation is not trivial. Adjacently cut tissue sections are only of limited use as one has to rely on cellular structures to be larger than 10 μm, the normal tissue thickness for SXRF samples. One approach is described by Miller et al., who used synchrotron Fourier transform infrared micro-spectroscopy (FTIRM) to correlate the location of senile plaques in the brains of human subjects with Alzheimer's disease to the distribution of metals in these brains (Miller et al. 2006). Another approach was suggested by Pickering et al. who used optical photographs to localize the 2-D distribution of arsenic or selenium to different regions of plants (Pickering et al. 2006, 2000).

Modern, high resolution SXRF utilizes beam sizes $\leq$500 nm. To obtain information about distributions of elements with cellular compartments, correlation techniques should closely match this resolution and should be applied to the same piece of tissue either before (in case of light differential interference contrast microscopy, DIC) or after the SXRF measurement (any type of histological staining). DIC or optical images are routinely published alongside the 2-D elemental distributions generated by SXRF but these images rarely provide information beyond cellular boundaries, and so far, have not yielded any necessary subcellular information (Finney et al. 2007). To visualize subcellular organelles in SXRF images of a single cell, McRae et al. employed organelle specific antibodies that were conjugated to colloidal gold particles (McRae et al. 2006). The gold is detected by SXRF (at the Au-L1 edge) along with other elements, and subsequent overlay of gold distribution with that of other elements revealed the location of labeled compartments and their elemental content. Using this elegant method McRae et al. were able to determine the elemental distribution for copper and zinc in the Golgi apparatus and the mitochondria of fibroblasts (McRae et al. 2006).

An alternative approach to identification of cellular compartments in cells and tissues is to use intrinsic differences in the elemental composition and sizes of organelles. For example, our own SXRF

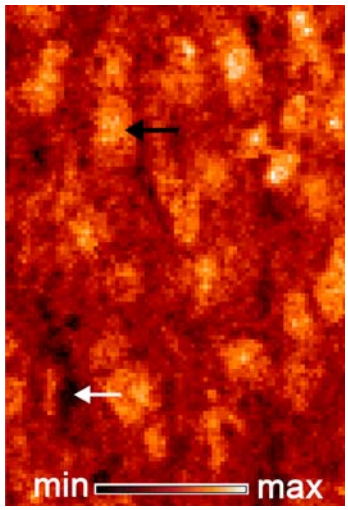

Fig. 2 2-D elemental map for potassium of a wild type mouse liver section. The nuclei are clearly visible as brightest area (*black arrow*) while the cytosol is represented by the slightly darker, surrounding regions. The black regions are empty spaces (*white arrow*). The bar at the bottom of the image shows the false color display for the concentration range (red-temperature scale)

experiments demonstrated that in mouse hepatocytes, phosphorous and potassium are on average more abundant compared to the cytosol (15–25% and 8–15%, respectively). This is illustrated in Fig. 2: nuclei show a higher than average fluorescent intensity for potassium (black arrow) while empty spaces such as sinusoids or bile canaliculi are recognized by a sharp decrease in fluorescent counts for all elements (white arrow).

Tissue preparation for the SXRF imaging

Proper preparation of tissues for high resolution SXRF imaging is crucial in order to take full advantage of the capabilities provided by the high brilliance of the X-ray beam at high photon energy. The window of a sample holder, on which the sample is deposited prior to scanning, has to be made of a material that does not contain elements that will be measured in the sample and it has to be free from impurities. Si_3N_4 windows or gold grids as used in electron microscopy satisfy these requirements and are widely employed as sample support in SXRF (Finney et al. 2007; McRae et al. 2006; Twining et al. 2003; Yang et al. 2005).

The size of these supports is the limiting factor of the area that can be imaged (usually 2 × 2 mm). The choice of window material depends on the type of the correlative methods to be applied to the sample before or after the SXRF experiment. For example, to be able to correlate the SXRF data with IR spectroscopy results Miller et al. used a suprasil quartz microscope slide that was sputtered with a thin layer of aluminum as a sample substrate (Miller et al. 2006). Our group is interested in the imaging copper distribution in healthy and diseased livers. In addition to using differences in potassium and phosphorus concentrations within the cell (see above), we stain samples after SXRF scanning with either hematoxylin and eosin (H&E) to visualize cell morphology or with immunohistochemical markers to better identify cell compartments (Ralle et al. submitted). To be able to work with the tissue after the SXRF experiment we needed window support material that could be easily attached to the sample holder and then equally well detached after completion of the experiment. Another requirement was to be able to scan larger pieces of tissues to better determine the macroscopic liver morphology (i.e. to visualize the three zones in liver accinus). Lastly, we needed to have sample holders that were easy to handle in the cryostat where sectioning of the tissue takes place. As a result we developed the lucite sample holder shown in Fig. 3 to

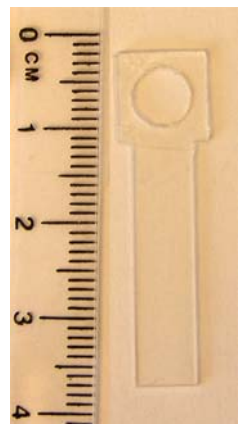

Fig. 3 Sample holder designed for SXRF and histology analysis of tissue samples. Sample holders were designed to work with the sample mount at APS. The larger than normal window area allows for large area scanning of tissues. The window material (Ultralene, SpexSampleprep) is attached to the sample holder with nail polish. The sample holders were machined by Huffstetter machining, Hillsboro, OR

which thin film material (4 micron Ultralene) is attached by nail polish.

To ensure proper preservation of tissue morphology, handling of tissue prior to SXRF scanning has to be kept to a minimum. Formalin fixed tissue has excellent morphology and can be used for SXRF experiments, however this procedure will produce reliable results only for tightly bound ions such as copper and iron; prolonged storage in formalin solution will lead to the loss of all diffusible elements. We have found that an alternative strategy can produce good quality results. When fresh, saline-perfused tissue is embedded in an OCT (optimum cutting temperature) compound and subsequently flash-frozen in dry ice-cooled isopentane the tissue retains its morphology almost entirely. The OCT embedded block is sectioned in a cryostat and the morphology accessed from an adjacently cut, H&E stained section. Air-drying of tissue sample will result in only little distortion of the sample topology and cause some tearing but does not destroy the overall morphology of tissue.

Future applications of SXRF imaging

SXRF imaging is the ideal and, so far, the only tool to reliably determine elemental distribution in tissue samples at the subcellular level with high sensitivity and low background. With optimized protocols for sample preparation and correlative techniques in place, all necessary tools are now available to investigate fundamental problems related to metal content of tissues. It is certain that SXRF will significantly contribute to the study of metallomes in different organisms, from plants to humans. However, SXRF is not a routine spectroscopic method and is not suitable for analysis of large numbers of samples because of the scarcity of available synchrotron sources. The amount of data that can be collected during a typical user cycle is limited by the scan speed and desired resolution. The scan speed (the time the detector spends at each point on a sample) is determined by the time it takes to collect a sufficient amount of photons. The resolution is dependent on the available focusing optics. However, often the deciding factor when choosing the resolution for a scan is the total scan time (higher resolution = longer scan time). Users have to choose what size scan at which resolution and scan speed will result in sufficient data collection given the limited amount of beamtime. The time it takes to scan a sample at a given resolution is ultimately determined by the brilliance of the focused beam at high photon energy and will only significantly improve if the brilliance of the beam is improved. Thus, SXRF is likely to help when important biological questions about metal ion distribution, concentration, and oxidation state need to be answered and only small amounts of materials are available (such as biopsy samples) while resolution of individual cells (or their compartments) is critical.

Acknowledgments The authors would like to gratefully acknowledge the use of the facilities at the Advanced Photon Source. This work was supported by a National Institutes of Health Grant GM067166 to SL, the use of the Advanced Photon Source was supported by the U.S. Department of Energy, Office of Science Contract DE-AC-02-06CH11357

References

Ala A, Walker AP, Ashkan K, Dooley JS, Schilsky ML (2007) Wilson's disease. Lancet 369:397–408. doi:10.1016/S0140-6736(07)60196-2

Becker JS, Mounicou S, Zoriy MV, Becker JS, Lobinski R (2008) Analysis of metal-binding proteins separated by non-denaturating gel electrophoresis using matrix-assisted laser desorption/ionization mass spectrometry (MALDI-MS) and laser ablation inductively coupled plasma mass spectrometry (LA-ICP-MS). Talanta 76:1183–1188. doi:10.1016/j.talanta.2008.05.023

Becker JS, Zoriy M, Becker JS, Pickhardt C, Damoc E, Juhacz G, Palkovits M, Przybylski M (2005) Determination of phosphorus-, copper-, and zinc-containing human brain proteins by LA-ICPMS and MALDI-FTICR-MS. Anal Chem 77:5851–5860. doi:10.1021/ac0506579

Buiakova OI, Xu J, Lutsenko S, Zeitlin S, Das K, Das S, Ross BM, Mekios C, Scheinberg IH, Gilliam TC (1999) Null mutation of the murine ATP7B (Wilson disease) gene results in intracellular copper accumulation and late-onset hepatic nodular transformation. Hum Mol Genet 8:1665–1671. doi:10.1093/hmg/8.9.1665

Choi DW, Koh JY (1998) Zinc and brain injury. Annu Rev Neurosci 21:347–375. doi:10.1146/annurev.neuro.21.1.347

Danks DM, Campbell PE, Stevens BJ, Mayne V, Cartwright E (1972) Menkes's kinky hair syndrome. An inherited defect in copper absorption with widespread effects. Pediatrics 50:188–201

Dillon CT, Lay PA, Kennedy BJ, Stampfl AP, Cai Z, Ilinski P, Rodrigues W, Legnini DG, Lai B, Maser J (2002) Hard X-ray microprobe studies of chromium(VI)-treated V79 Chinese hamster lung cells: intracellular mapping of the biotransformation products of a chromium carcinogen.

J Biol Inorg Chem 7:640–645. doi:10.1007/s00775-002-0343-5

Finney L, Mandava S, Ursos L, Zhang W, Rodi D, Vogt S, Legnini D, Maser J, Ikpatt F, Olopade OI, Glesne D (2007) X-ray fluorescence microscopy reveals large-scale relocalization and extracellular translocation of cellular copper during angiogenesis. Proc Natl Acad Sci USA 104:2247–2252. doi:10.1073/pnas.0607238104

Hall MD, Dillon CT, Zhang M, Beale P, Cai Z, Lai B, Stampfl AP, Hambley TW (2003) The cellular distribution and oxidation state of platinum(II) and platinum(IV) antitumour complexes in cancer cells. J Biol Inorg Chem 8:726–732. doi:10.1007/s00775-003-0471-6

Hanaichi T, Kidokoro R, Hayashi H, Sakamoto N (1984) Electron probe X-ray analysis on human hepatocellular lysosomes with copper deposits: copper binding to a thiol-protein in lysosomes. Lab Invest 51:592–597

Harris HH, Levina A, Dillon CT, Mulyani I, Lai B, Cai Z, Lay PA (2005) Time-dependent uptake, distribution and biotransformation of chromium(VI) in individual and bulk human lung cells: application of synchrotron radiation techniques. J Biol Inorg Chem 10:105–118. doi:10.1007/s00775-004-0617-1

Huster D, Finegold MJ, Morgan CT, Burkhead JL, Nixon R, Vanderwerf SM, Gilliam CT, Lutsenko S (2006) Consequences of copper accumulation in the livers of the atp7b$^{-/-}$ (Wilson disease gene) knockout mice. Am J Pathol 168:423–434. doi:10.2353/ajpath.2006.050312

Kemner KM, Kelly SD, Lai B, Maser J, O'Loughlin EJ, Sholto-Douglas D, Cai Z, Schneegurt MA, Kulpa CF Jr, Nealson KH (2004) Elemental and redox analysis of single bacterial cells by X-ray microbeam analysis. Science 306:686–687. doi:10.1126/science.1103524

Kirz J, Sayre D, Dilger J (1978) Short Wavelength Microscopy. NY Academy of Science, New York

Koh JY, Suh SW, Gwag BJ, He YY, Hsu CY, Choi DW (1996) The role of zinc in selective neuronal death after transient global cerebral ischemia. Science 272:1013–1016. doi:10.1126/science.272.5264.1013

Lahner B, Gong J, Mahmoudian M, Smith EL, Abid KB, Rogers EE, Guerinot ML, Harper JF, Ward JM, McIntyre L, Schroeder JI, Salt DE (2003) Genomic scale profiling of nutrient and trace elements in Arabidopsis thaliana. Nat Biotechnol 21:1215–1221. doi:10.1038/nbt865

Loudianos G, Gitlin JD (2000) Wilson's disease. Semin Liver Dis 20:353–364. doi:10.1055/s-2000-9389

McCrea RP, Harder SL, Martin M, Buist R, Nichol H (2008) A comparison of rapid-scanning X-ray fluorescence mapping and magnetic resonance imaging to localize brain iron distribution. Eur J Radiol 68:109–113

McRae R, Lai B, Vogt S, Fahrni CJ (2006) Correlative microXRF and optical immunofluorescence microscopy of adherent cells labeled with ultrasmall gold particles. J Struct Biol 155:22–29. doi:10.1016/j.jsb.2005.09.013

Miller LM, Wang Q, Telivala TP, Smith RJ, Lanzirotti A, Miklossy J (2006) Synchrotron-based infrared and X-ray imaging shows focalized accumulation of Cu and Zn co-localized with beta-amyloid deposits in Alzheimer's disease. J Struct Biol 155:30–37

Nakazato K, Nagamine T, Suzuki K, Kusakabe T, Moon HD, Oikawa M, Sakai T, Arakawa K (2008) Subcellular changes of essential metal shown by in-air micro-PIXE in oral cadmium-exposed mice. Biometals 21:83–91. doi:10.1007/s10534-007-9095-6

Paunesku T, Rajh T, Wiederrecht G, Maser J, Vogt S, Stojicevic N, Protic M, Lai B, Oryhon J, Thurnauer M, Woloschak G (2003) Biology of TiO2-oligonucleotide nanocomposites. Nat Mater 2:343–346. doi:10.1038/nmat875

Pickering IJ, Gumaelius L, Harris HH, Prince RC, Hirsch G, Banks JA, Salt DE, George GN (2006) Localizing the biochemical transformations of arsenate in a hyperaccumulating fern. Environ Sci Technol 40:5010–5014. doi:10.1021/es052559a

Pickering IJ, Prince RC, Salt DE, George GN (2000) Quantitative, chemically specific imaging of selenium transformation in plants. Proc Natl Acad Sci USA 97:10717–10722. doi:10.1073/pnas.200244597

Roomans GM (1988) Introduction to X-ray microanalysis in biology. J Electron Microsc Tech 9:3–17. doi:10.1002/jemt.1060090103

Roomans GM, Von Euler A (1996) X-ray microanalysis in cell biology and cell pathology. Cell Biol Int 20:103–109. doi:10.1006/cbir.1996.0014

Sham TK, Kim PSG, Ngo H, Chakrabarti S, Adams PC (2005) X-ray Microspectroscopy of Hemochromatosis Liver and Diabetic Mice Kidney Tissues: Preliminary Observations. Phys Scr T 115:1047–1049. doi:10.1238/Physica.Topical.115a01047

Sparks CJ (1980) Synchrotron Radiation Research. Plenum Press, New York

Szokefalvi-Nagy Z (1994) Applications of PIXE in the life sciences. Biol Trace Elem Res 43–45:73–78. doi:10.1007/BF02917301

Twining BS, Baines SB, Fisher NS, Maser J, Vogt S, Jacobsen C, Tovar-Sanchez A, Sanudo-Wilhelmy SA (2003) Quantifying trace elements in individual aquatic protist cells with a synchrotron X-ray fluorescence microprobe. Anal Chem 75:3806–3816. doi:10.1021/ac034227z

Van Espen P (2002) Spectrum Evaluation Handbook of X-ray Spectrometry. Marcel Dekker, New York

Vogt S (2003) Maps: A set of software tools for analysis and visualization of 3D X-ray fluorescent datasets. J Phys IV 104:635–638. doi:10.1051/jp4:20030160

Waern JB, Harris HH, Lai B, Cai Z, Harding MM, Dillon CT (2005) Intracellular mapping of the distribution of metals derived from the antitumor metallocenes. J Biol Inorg Chem 10:443–452. doi:10.1007/s00775-005-0649-1

Waggoner DJ, Bartnikas TB, Gitlin JD (1999) The role of copper in neurodegenerative disease. Neurobiol Dis 6:221–230. doi:10.1006/nbdi.1999.0250

Yang L, McRae R, Henary MM, Patel R, Lai B, Vogt S, Fahrni CJ (2005) Imaging of the intracellular topography of copper with a fluorescent sensor and by synchrotron X-ray fluorescence microscopy. Proc Natl Acad Sci USA 102:11179–11184. doi:10.1073/pnas.0406547102

Yun W, Lai B, Cai Z, Maser J, Legnini D, Gluskin E, Chen Z, Krasnoperova A, Valdimirsky Y, Cerrina F, Di Fabrizio E, Gentili M (1999) Nanometer Focusing of Hard X-Rays

by Phase Zone Plates. Rev Sci Instrum 70:2238–2241. doi:10.1063/1.1149744

Zierold K (2000) Heavy metal cytotoxicity studied by electron probe X-ray microanalysis of cultured rat hepatocytes. Toxicol In Vitro 14:557–563. doi:10.1016/S0887-2333(00)00049-7